physica status solidi b
www.pss-b.com

On the Possibility of Realizing a 2D Structure of Si—N Bonds by Metal-Organic Chemical Vapor Deposition

*Béla Pécz, Miklos Nemeth, Filippo Giannazzo, and Anelia Kakanakova-Georgieva**

2D SiN honeycomb monolayer structures predicted theoretically have been the focus of interest in materials science for a long time, most recently for their semiconducting and ferromagnetic properties. Herein, by investigating metal-organic chemical vapor deposition processes and direct heat treatment of epitaxial graphene in ammonia flow, the possibility of realizing a certain periodic 2D structure via Si—N bonds under epitaxial graphene on SiC (0001) is reported. The result is of interest because it is compatible with semiconductor material deposition technologies and future use in nanoscience and nanotechnology.

1. Introduction

Early reports of AlN epitaxial layers heavily doped with silicon by metal-organic chemical vapor deposition (MOCVD) used the formation of a submonolayer coverage through bonds between silicon (Si) and nitrogen (N) atoms to explain the formation of facets in their microstructure.[1] In general, MOCVD of AlN implements precursors such as ammonia (NH_3) and trimethylaluminum ($(CH_3)_3Al$), and a dopant precursor such as silane (SiH_4). During SiH_4 delivery, AlN (0001) surface interactions at N dangling bond sites are perceived to promote Si—N bond formation and stabilization of {1-101} facets.[1] A coverage of Si—N bonds can also be formed as a result of a characteristic surface treatment of the GaN (0001) surface with a flush of silane or tetraethylsilicon precursor to produce a Si δ-doped layer.[2,3] The structure and composition of this very thin (≈1 nm) layer was investigated by transmission electron microscopy (TEM).[2,3] It was concluded that this layer is a crystalline Si-compound phase and that its crystal structure has a lattice conformation to GaN.[2] By using high-resolution aberration-corrected transmission electron microscopy and in combination with ab initio calculations and imaging simulations, the atomic structure of this layer was further identified as a monolayer of $SiGaN_3$, where the three cationic positions in the unit cell are occupied by either Si_{Ga}, V_{Ga}, or Ga.[3]

In recent years, a focus has been placed on MOCVD of AlN and GaN films on epitaxial graphene formed by thermal decomposition of SiC at elevated temperatures and various other graphene-coated substrates, drawing attention to even more distinctive growth characteristics. These growth characteristics are related to the surface interactions of the ammonia precursor with the graphene lattice and the formation of sp^2 C—N and sp^3 C—N bonding.[4–10] The sp^2 C—N and sp^3 C—N bonding is considered the result from the incorporation of nitrogen defects into the graphene lattice by its exposure to ammonia, which promotes the nucleation of AlN and GaN on graphene. Often, graphene samples were first treated with an O_2[4] or nitrogen N_2[6,8] plasma to increase the density of defect sites in the graphene lattice and its reactivity.

Here, by investigating MOCVD processes and direct heat treatment of epitaxial graphene in ammonia flow, we report the possibility of realizing a 2D structure through Si—N bonds underneath epitaxial graphene on SiC (0001).

2. Results and Discussion

A high-resolution transmission electron microscopy (HRTEM) study of the graphene/SiC interface heated in a flow of ammonia reveals how graphene can be resolved parallel to the surface (**Figure 1**a). The graphene layers can be clearly seen and are obviously displaced from the SiC surface. Their local fragmentation is also observed from the image of individual graphene layers showing discontinuity. This type of structural features of graphene was previously reported in connection with the functionalization of graphene from a precursor such as trimethylaluminum.[11]

The main feature of the HRTEM image is the laterally homogeneous row of evenly spaced, 4.7 Å, bright spots located immediately on the surface of the SiC substrate (Figure 1b). The distance of 4.7 Å was measured by the intensity profile

B. Pécz, M. Nemeth
Centre for Energy Research
Institute for Technical Physics and Materials Science
Konkoly-Thege M. út 29-33., 1121 Budapest, Hungary

F. Giannazzo
Consiglio Nazionale delle Ricerche
Istituto per la Microelettronica e Microsistemi
Strada VIII, n. 5, Zona Industriale, I-95121 Catania, Italy

A. Kakanakova-Georgieva
Division of Semiconductor Materials
Department of Physics
Chemistry and Biology (IFM)
Linköping University
SE-58183 Linköping, Sweden
E-mail: anelia.kakanakova@liu.se

The ORCID identification number(s) for the author(s) of this article can be found under https://doi.org/10.1002/pssb.202300262.

DOI: 10.1002/pssb.202300262

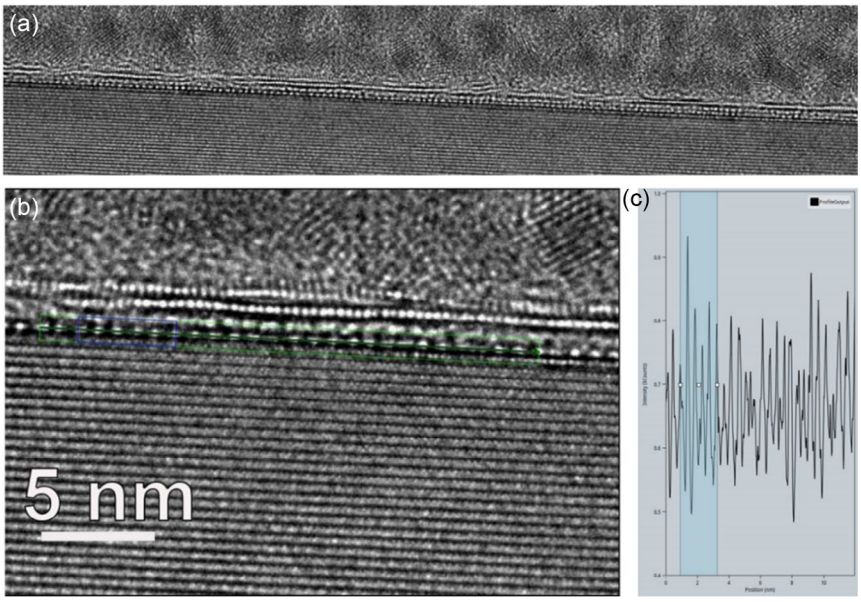

Figure 1. a) A region from the ammonia intercalated graphene/SiC interface viewed from the (10-10) section, where the graphene is resolved parallel to the interface; b) magnified part with a measuring bar; the green bar is used for measuring c) intensity profile.

(Figure 1c). We compare this distance with the periodic contrast of an atomic structure model of a Si—N layer previously reported in ref. [12]. This atomic structure model was obtained from HRTEM and in combination with density functional theory (DFT) calculations and image simulations applied to the interlayer between zero-layer graphene and SiC substrate.[12] We note that the atomic model of this periodic 2D Si—N structure is different from the 2D honeycomb network of Si and N atoms with optimized lattice constants, as reported, for example, in refs. [13,14]. The 2D honeycomb network of Si and N atoms is usually modeled as a free-standing sheet. In contrast, a common feature between the experimentally confirmed periodic 2D structure of Si—N bonds in this study as well as in ref. [12] is its confinement at the graphene/SiC interface.

The interfacial 2D structure of Si—N bonds reported in ref. [12] was the result of a special treatment of the SiC surface prior to the formation of graphene, i.e., consists of heating the SiC substrate at a high temperature of 1600 °C in a 3 atm N_2/Ar static gas mixture. The formation of the 2D structure of Si—N bonds in our study results from a postgrowth treatment of epitaxial graphene and its thermal reaction with ammonia under MOCVD conditions typical of AlGaN growth on SiC. The formation of the 2D structure of Si—N bonds in our study suggests the occurrence of N intercalation at the graphene/SiC interface and its bonding to the topmost Si atoms on the SiC surface, adopting a certain periodic atomic pattern. The occurrence of the N intercalation at the graphene/SiC interface should be directly related to the dissociative adsorption of the NH_3 precursor, respectively, to the surface reactions of the NH_3 precursor with graphene in the applied MOCVD conditions. The atomic-scale mechanisms that govern these reactions, and any other precursor/surface reactions in MOCVD processes in general, are largely unknown. We applied ab initio molecular dynamics (AIMD) simulations as an indispensable tool to identify the reaction pathways responsible for the dissociation of a precursor such as trimethylindium on top-layer and zero-layer graphene on SiC,[15] as well as trimethylaluminum and NH_3 precursors on defect-free free-standing graphene.[16] In the latter case, AIMD simulations provided plausible interpretations of atomistic and electronic processes responsible for the delivery of aluminum adatoms onto pristine graphene via precursor/surface reactions.[16] Unlike trimethylaluminum, the dissociative adsorption of NH_3 and ultimately the ability to deliver nitrogen atoms to the graphene surface is expected to occur on the graphene surface in the presence of other species[17] or at defect sites.[18] In particular, AIMD simulations to study the interaction of the NH_3 precursor with graphene of various structures involving defects such as Stone–Wales, single as well as divacancy were reported in ref. [18].

The high thermal stability of NH_3 (N—H bond strength of 3.9 eV),[19] although still low compared to N_2 (N—N bond strength of 9.5 eV), indeed suggests that its dissociative adsorption on the graphene surface should be greatly facilitated by structural defects that can offer chemically active dangling bonds.

Figure 2a,b shows typical AFM morphology (with a surface root-mean-square (RMS) roughness of 1.25 nm) and phase images collected on the graphene surface, after heat treatment with NH_3. Besides the SiC substrate steps, regions with a specific hexagonal shape showing a lower height than the surrounding regions are seen in the surface morphology of epitaxial graphene (Figure 2a). These regions also show lower phase contrast than the surrounding areas (Figure 2b). A typical lateral size of ≈300 nm and depth of ≈0.65 nm of these features was deduced from the higher resolution morphological image in Figure 2c and the height linescan in Figure 2d. A representative AFM morphology and phase image of as-grown epitaxial graphene on on-axis 4H-SiC(0001) are shown in Figure S1, Supporting Information. The surface topography shows a lower roughness (RMS = 0.3 nm) mainly related to the SiC steps, while the phase image shows a uniform contrast, indicating uniform graphene coverage on the

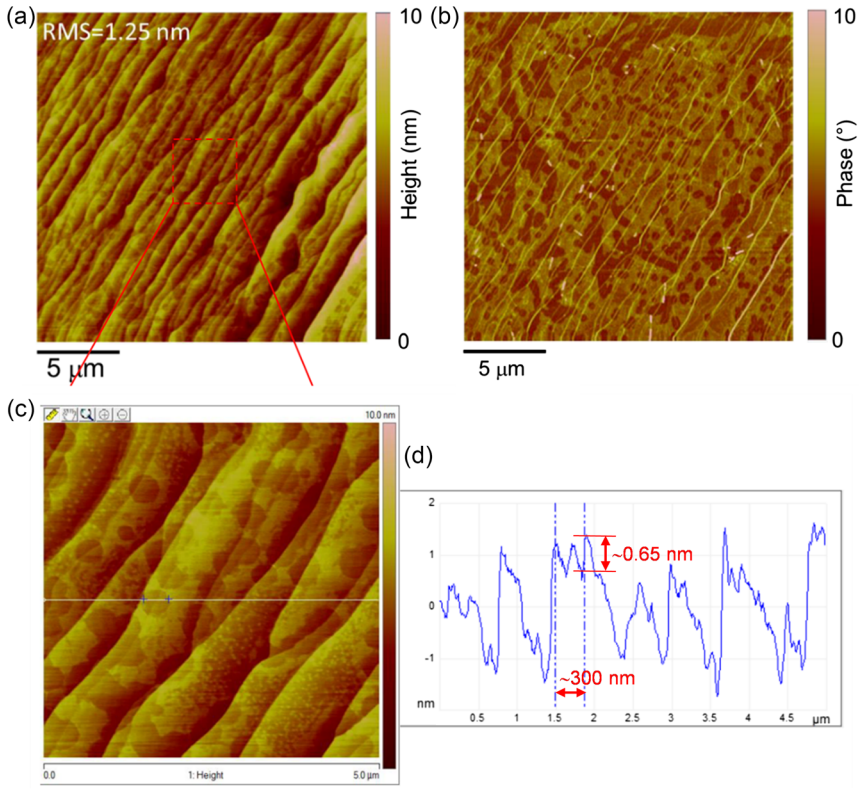

Figure 2. a) Tapping mode surface morphology and b) phase images of epitaxial graphene after heat treatment with NH_3. c) Higher resolution morphological map and d) height linescan showing typical hexagonal depressions in the surface (with lateral size ≈300 nm and depth of ≈0.65 nm), probably associated with etched graphene regions.

SiC surface. These AFM images serve for comparison with the AFM images of the NH_3-treated sample and show the extent of the morphological changes that occurred upon this treatment.

These regions may indicate the sites of local graphene disintegration/etching extending from topological defects that were originally incorporated into the as-grown graphene

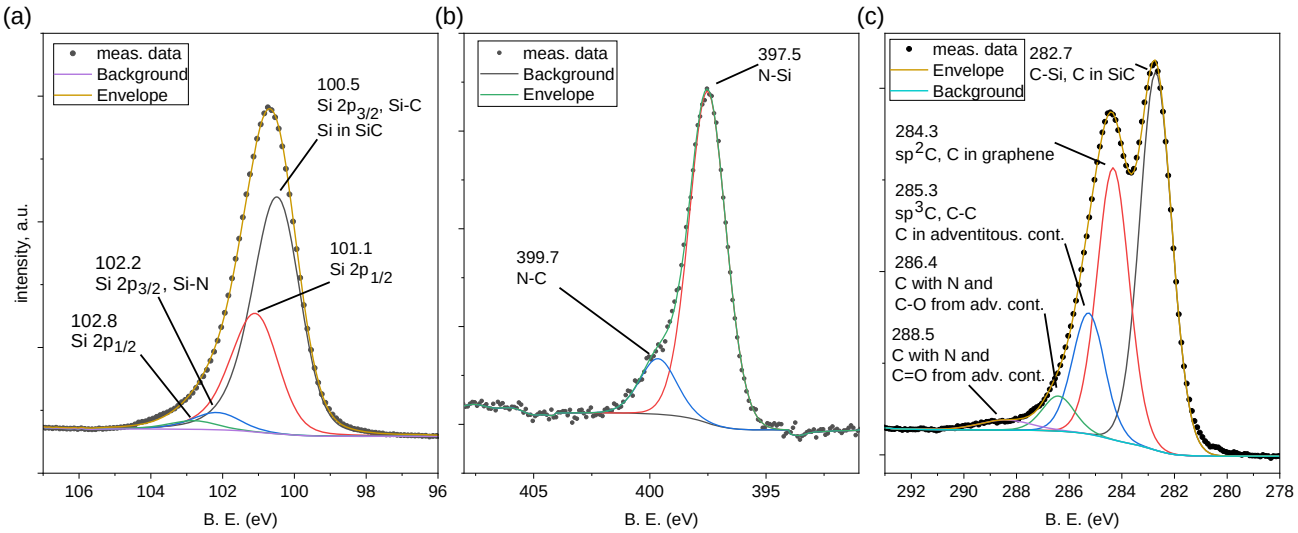

Figure 3. a) Si 2*p*, b) N 1s, and c) C 1s XPS spectra obtained after ammonia treatment of the graphene/SiC interface. Each of the Si 2*p*, N 1s, and C 1s spectra can be deconvoluted into several component peaks. The Si–C component of the Si $2p_{3/2}$ peak at 100.5 eV was used as a reference for charge compensation.[20] The component peak at 102.2 eV in the Si 2*p* spectrum is attributed to Si—N bond.[21,22] The component peak at 397.5 eV in the N 1s spectrum is attributed to N—Si bond.[23]

lattice. Such defects suggest the presence of chemically active dangling bonds that can support the dissociative adsorption of NH_3. Ultimately, a range of possible carbon dangling bond terminations with N, NH, or NH_2 can be expected in the distorted graphene structure.

The low intensity peaks at the high binding energy of 288.5 and 286.4 eV of the C 1*s* spectrum, **Figure 3**c, and at 399.7 eV of the N 1*s* spectrum, Figure 3b, indicate the presence of C—N bonds in the ammonia-treated graphene/SiC interface. A stricter interpretation of these peaks is hindered by the possibility of a contribution from adventitious contaminants. After peak fitting of the Si 2*p* spectrum, a component peak at 102.2 eV can be located. The position of the peaks at the binding energy of 102.2 eV of the Si 2*p* spectrum, Figure 3a, and at 397.5 eV of the N 1*s* spectrum confirms the formation of Si—N bonds.

The MOCVD reactor was operated at a pressure of 200 mbar with an H_2 flow rate of 6 slm and an NH_3 flow rate of 10 slm. Heat treatment of the graphene/SiC interface was performed at 1100 °C for 30 min. Due to the presence of H_2 carrier gas in the overall total flow, we performed a reference heat treatment of the graphene/SiC interface only in a H_2 flow of 25 slm at the same temperature of 1100 °C for 30 min. An XPS study was carried out on H_2- and NH_3-treated graphene/SiC interfaces to confirm the changes in core levels that occurred upon NH_3 treatment and Si—N bonding. The result of this study is presented in Figure S2, Supporting Information.

Exposure of graphene to ammonia in various postgrowth treatment approaches, including the MOCVD processes referred to in Introduction, has been established as an alternative mechanism for incorporating nitrogen atoms into the graphene lattice while causing different C—N bond types and their diverse effects on the electronic structure in N-doped graphene.

Here, we use epitaxial graphene thermally annealed in ammonia under MOCVD conditions to indicate a possibility of realizing a periodic 2D structure through Si—N bonds at the graphene/SiC interface. The result gains significance as it is compatible with semiconductor material deposition technologies and future use in nanoscience and nanotechnology. We note that another 2D structure via Si—N bonds in the form of a free-standing 2D honeycomb sheet, predicted theoretically, has been the focus of interest in materials science for a long time,[13] most recently for its semiconducting and ferromagnetic properties.[14]

3. Experimental Section

MOCVD processes were performed in a horizontal-type hot-wall MOCVD reactor (GR508GFR Aixtron) using epitaxial graphene on a nominally on-axis 4H-SiC (0001) substrates. The reactor was operated at a pressure of 200 mbar with an H_2 flow rate of 6 slm and an NH_3 flow rate of 10 slm. Heat treatment of the graphene sample was performed at 1100 °C for 30 min. The epitaxial graphene was grown by high-temperature thermal decomposition of the Si-face 4H-SiC bulk substrate in an argon atmosphere.[24] The as-grown epitaxial graphene applied in this study was a monolayer coverage with bilayer patches associated with surface steps. Surface steps are typical of these substrates as they relate to the unintentional misorientation of the SiC substrate that occurs during substrate fabrication. A reflectance map of as-grown epitaxial graphene was reported in connection with one of our previous studies (see Figure S1 in ref. [25]). Tapping mode atomic force microscopy (AFM) analyses (morphology and phase imaging) were carried out with a DI3100 equipment by Bruker, using ultrasharp silicon tips (nominal curvature radius <5 nm). X-ray photoelectron spectroscopy (XPS) was used to investigate the surface composition of the samples and performed on a KRATOS XSAM 800 XPS instrument. The samples were analyzed using a non-monochromatized Al K-alpha source (1486.6 eV). All measurements were performed in the fixed analyzer transmission (FAT) mode. Wide range spectra (at an analyzer pass energy of 80 eV) were collected on each sample for surveying the elemental composition. The pass energy of the hemispherical analyzer was set at 40 eV to record the high-resolution spectra of the C 1s, N 1s, and Si 2*p* regions. A Shirley-type baseline was used for all peak fits and spectral components were fitted using a GL(30) line shape. TEM lamella was cut by a focused ion beam (FIB) in which the Ga ion energy was reduced to 2 keV in a Thermo Fisher Scientific SCIOS2 dual-beam equipment and observations were performed in an Thermo Fisher Scientific THEMIS 200 microscope equipped with an image corrector at 200 keV.

Supporting Information

Supporting Information is available from the Wiley Online Library or from the author.

Acknowledgements

The authors thank Dr. T. Iakimov and Prof. R. Yakimova for kindly providing samples of epitaxial graphene. A.K.-G. acknowledges support from the Swedish Research Council under VR2017-04071. B.P. acknowledges funding from the national projects TKP2021-NKTA-05 and VEKOP-2.3.3-15-2016-00002. F.G. and B.P. acknowledge funding from the CNR-HAS 2022-25 bilateral project GHOST III.

Conflict of Interest

The authors declare no conflict of interest.

Data Availability Statement

The data that support the findings of this study are available from the corresponding author upon reasonable request.

Keywords

ammonia, graphene, metal-organic chemical vapor deposition, silicon nitride

Received: June 9, 2023
Revised: July 11, 2023
Published online: August 16, 2023

[1] M. Kasu, N. Kobayashi, *Appl. Phys. Lett.* **2001**, *78*, 1835.
[2] N. Kuwano, M. Hijikuro, S. Hata, M. Takeuchi, Y. Aoyagi, *J. Cryst. Growth* **2007**, *298*, 284.
[3] T. Markurt, L. Lymperakis, J. Neugebauer, P. Drechsel, P. Stauss, T. Schulz, T. Remmele, V. Grillo, E. Rotunno, M. Albrecht, *Phys. Rev. Lett.* **2013**, *110*, 036103.
[4] Z. Y. Al Balushi, T. Miyagi, Y.-C. Lin, K. Wang, L. Calderin, G. Bhimanapati, J. M. Redwing, J. A. Robinson, *Surf. Sci.* **2015**, *634*, 81.
[5] G. Sarau, M. Heilmann, M. Bashouti, M. Latzel, C. Tessarek, S. Christiansen, *ACS Appl. Mater. Interfaces* **2017**, *9*, 10003.

[6] Z. Chen, Z. Liu, T. Wei, S. Yang, Z. Dou, Y. Wang, H. Ci, H. Chang, Y. Qi, J. Yan, J. Wang, Y. Zhang, P. Gao, J. Li, Z. Liu, *Adv. Mater.* **2019**, *31*, 1807345.
[7] Y. Feng, X. Yang, Z. Zhang, D. Kang, J. Zhang, K. Liu, X. Li, J. Shen, F. Liu, T. Wang, P. Ji, F. Xu, N. Tang, T. Yu, X. Wang, D. Yu, W. Ge, B. Shen, *Adv. Funct. Mater.* **2019**, *29*, 1905056.
[8] Y. Wang, S. Yang, H. Chang, W. Lia, X. Chen, R. Hou, J. Yan, X. Yi, J. Wang, T. Wei, *Appl. Surf. Sci.* **2020**, *520*, 146358.
[9] Y. Chen, H. Zang, K. Jiang, J. Ben, S. Zhang, Z. Shi, Y. Jia, W. Lu, X. Sun, D. Li, *Appl. Phys. Lett.* **2020**, *117*, 051601.
[10] J.-H. Park, X. Yang, J.-Y. Lee, M.-D. Park, S.-Y. Bae, M. Pristovsek, H. Amano, D.-S. Lee, *Chem. Sci.* **2021**, *12*, 7713.
[11] A. Kakanakova-Georgieva, G. K. Gueorguiev, D. G. Sangiovanni, N. Suwannaharn, I. G. Ivanov, I. Cora, B. Pécz, G. Nicotra, F. Giannazzo, *Nanoscale* **2020**, *12*, 19470.
[12] Y. Masuda, W. Norimatsu, M. Kusunoki, *Phys. Rev. B* **2015**, *91*, 075421.
[13] T. He, M. Zhao, W. Li, C. Song, X. Lin, X. Liu, Y. Xia, L. Mei, *J. Phys. Chem. C* **2007**, *111*, 16840.
[14] N. V. Tkachenko, B. Song, D. Steglenko, R. M. Minyaev, L.-M. Yang, A. I. Boldyrev, *Phys. Status Solidi B* **2020**, *257*, 1900619.
[15] D. G. Sangiovanni, G. K. Gueorguiev, A. Kakanakova-Georgieva, *Phys. Chem. Chem. Phys.* **2023**, *25*, 829.
[16] D. G. Sangiovanni, R. Faccio, G. K. Gueorguiev, A. Kakanakova-Georgieva, *Phys. Chem. Chem. Phys.* **2018**, *20*, 17751.
[17] V. V. Chaban, O. V. Prezhdo, *J. Phys. Chem. Lett.* **2015**, *6*, 4397.
[18] X.-F. Li, K.-Y. Lian, L. Liu, Y. Wu, Q. Qiu, J. Jiang, M. Deng, Y. Luo, *Sci. Rep.* **2016**, *6*, 23495.
[19] O. Ambacher, *J. Phys. D: Appl. Phys.* **1998**, *31*, 2653.
[20] K. V. Emtsev, F. Speck, Th. Seyller, L. Ley, J. D. Riley, *Phys. Rev. B* **2008**, *77*, 155303.
[21] Z. Fang, *Surf. Coat. Technol.* **2008**, *202*, 4198.
[22] E. Ravizza, S. Spadoni, R. Piagge, P. Comitea, C. Wiemer, *Surf. Interface Anal.* **2012**, *44*, 120.
[23] I. Bertoti, *Surf. Coat. Technol.* **2002**, *151*, 194.
[24] R. Yakimova, T. Iakimov, M. Syväjärvi, US Patent US9150417B244, **2015**.
[25] A. Kakanakova-Georgieva, I. G. Ivanov, N. Suwannaharn, C.-W. Hsu, I. Cora, B. Pécz, F. Giannazzo, D. G. Sangiovanni, G. K. Gueorguiev, *CrystEngComm* **2021**, *23*, 385.